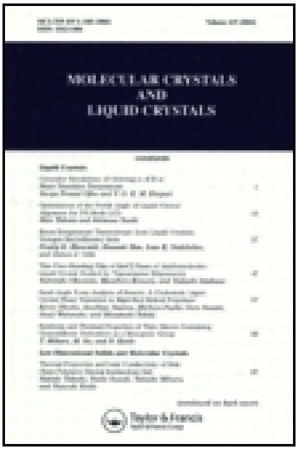

Molecular Crystals and Liquid Crystals Science and Technology. Section A. Molecular Crystals and Liquid Crystals

Publication details, including instructions for authors and subscription information:
http://www.tandfonline.com/loi/gmcl19

Dynamical Properties of Flexo Electric Effect in CCH Nematic Liquid Crystal

Y. Mieda [a] & N. Maruyama [a]

[a] Department of Applied Physics and Chemistry, The University of Electro-Communications, Chofugaoka 1-5-1, Chofu, Tokyo, 182-8585, JAPAN

Version of record first published: 12 Jun 2011

To cite this article: Y. Mieda & N. Maruyama (2001): Dynamical Properties of Flexo Electric Effect in CCH Nematic Liquid Crystal, Molecular Crystals and Liquid Crystals Science and Technology. Section A. Molecular Crystals and Liquid Crystals, 367:1, 25-35

To link to this article: http://dx.doi.org/10.1080/10587250108028620

Mol. Cryst. and Liq. Cryst., 2001, Vol. 367, pp. 25-35
Reprints available directly from the publisher
Photocopying permitted by license only

Dynamical Properties of Flexo Electric Effect in CCH Nematic Liquid Crystal

Y. MIEDA and N. MARUYAMA

Department of Applied Physics and Chemistry, The University of Electro-Communications, Chofugaoka 1–5–1, Chofu, Tokyo 182–8585, JAPAN

The flexo-electric effect of CCH nematic liquid crystal based on the splay deformation of wedge like molecules in Meyers model are investigated by the experimental techniques of interdigital electrode methods. Experimental results are analyzed by revised Jones matrix and are compared with numerical simulation based on continuum theory. In conclusion splay type flexoelectric effect themselves destroy linearity of flexoelectric effect in strong electric field region.

Keywords: flexoelectricity; nematic; splay mode; interdigital electrode

1 INTRODUCTION

Since a fundamental idea of flexoelectric effect for nematic liquid crystals was introduced by R. B. Meyer in 1969 [1], many attempts to demonstrate nature of this new effect had been proposed [2-3]. Unfortunately almost all experimental results were not ambiguous proof of the existence of flexoelectric effect, because separation of dielectric effect was not distinctly considered.

In 1976 J. Prost and P. S. Pershan succeeded ambiguous separation of dynamical properties of flexoelectric and dielectric effects by using of the interdigital electrode method [4]. Currently this method is one of the most elegant technique to measure flexoelectric and dielectric effects in nematic liquid crystals.

Using this method, we have precisely investigated splay type flexo-electrooptic effect of CCH-3 nematic liquid crystal. CCH-3 is one of the most simple suitable wedge like molecule in Meyer's model, because CN group has only large electric polarization in the direction of non aromatic cyclohexane hard core molecular long axis of and flexible alkyl chain (Fig. 1).

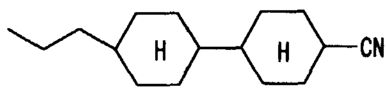

FIGURE 1. Molecular structure of CCH-3.

In this paper we report experimental results and especially applied electric field dependence. Experimental results are analyzed by revised Jones Matrix method and are compared with numerical simulation based on a continuum theory.

2 EXPERIMENTAL CONSIDERATIONS

Interdigital electrode method is the technique to measure selectively dynamical property of flexoelectric effect by Fraunhofer diffraction of light. According to modern lithographic techniques, it is easily possible to make a super fine electrode stripe pattern of $10^{-1}\,\mu$m order. So we selected most suitable electrode interval of d $=10\,\mu$m in this experiment for the highest quality alignment of monocrystalline homeotropic geometry and the sample thickness is $D = 25\,\mu$m.

In the applied electric fields, the expected responses of the periodic director pattern are linear and quadratic to flexoelectric and dielectric effects respectively. For normally incident laser beam (wave length λ) on the sample, both of the metallic electrodes themselves and the phase grating by dielectric effect diffract same direction of $\phi = \sin^{-1}(m\lambda/d)$ $(m=0, \pm 1, \pm 2, \cdots)$. Whereas the phase grating by flexoelectric effect diffract light peaks at $(m=0, \pm 0.5, \pm 1, \cdots)$. So if one select (m= ± 0.5, ± 1.5,···), then flexoelectric and dielectric effects are clearly separable from each other.

Fig. 2 illustrates block diagram of experimental setup.

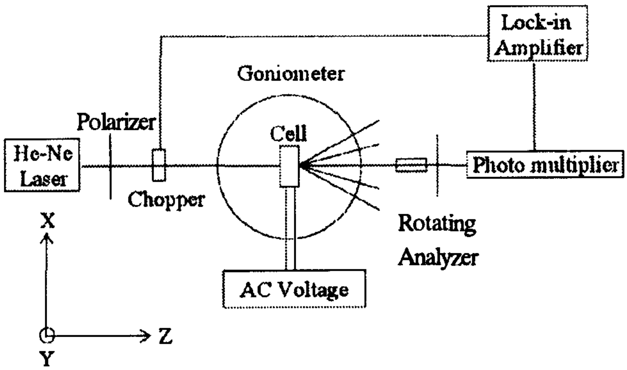

FIGURE 2. Block diagram of the experimental setup.

Sample is contained in electric heat oven, which the temperature was controlled to 10^{-3} °C. He-Ne laser (λ= 632.8 nm) passed through polarizer and the chopper is the incident light for the sample. Polarized direction for incident light is x direction. The scattered light is passed through analyzer and detected by photomultiplier. The exact measuring point is determined by x-ray Goniometer apparatus. The output signal of photomultiplier is fed into a lock-in amplifier in which the reference signal is locked to the chopper's frequency. By using rotating analyzer, light intensity for every rotation angle θ is measured automatically. The measuring point is (m = + 0.5). The frequency of applied AC voltage is selected 500 Hz, because the screening effect by ionic impurity are efficiently prevented.

Typical observations of the light intensity I (θ) for flexoelectric effects is shown in Fig. 3.

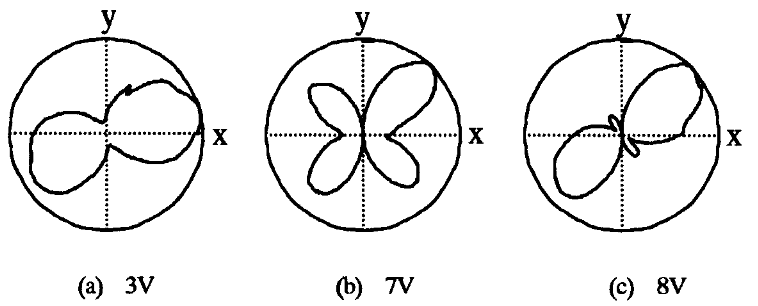

FIGURE 3. Examples of measured polarization characteristics of flexoelectric effect. The x-axis is Polarization direction of incident light. The light intensity of flexoelectric effect I (θ) is a function of analyzer rotating angle θ.

Polarization state of diffraction light from interdigital electrode cell is fairly complex, and these responses seem to have some character. To analyze the feature of these flexoelectric responses in Fig.3, $I(\theta)$ is expanded as a Fourier series $I(\theta) = \sum I(n)\exp(in\theta)$ (n=0,1,2, · · ·) (Fig. 4).

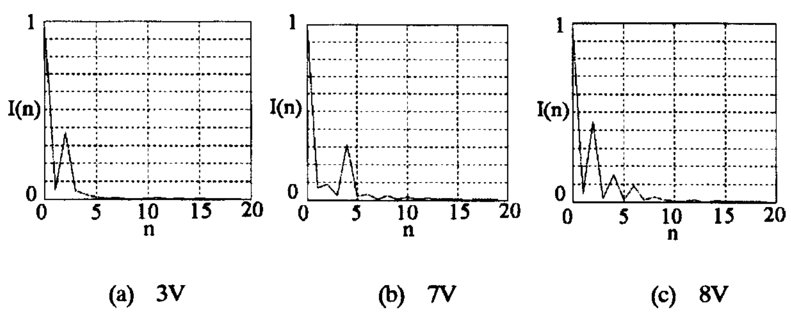

FIGURE 4. Fourier series expansion of I (θ),
$I(\theta) = \sum I(n)\exp(in\theta)$ (n=0,1,2, · · ·).

From Fig. 4, it was found that 4θ is essentially importance to flexo splay deformation.

We assume that Jones vector of passing through the analyzer is

$$\begin{pmatrix} E_x \\ E_y \end{pmatrix} = \begin{pmatrix} 1 & 0 \\ 0 & \rho \end{pmatrix} \begin{pmatrix} \cos\theta & -\sin\theta \\ \sin\theta & \cos\theta \end{pmatrix} \begin{pmatrix} 1 & 0 \\ 0 & 1 \end{pmatrix} \begin{pmatrix} \cos\theta & \sin\theta \\ -\sin\theta & \cos\theta \end{pmatrix} \begin{pmatrix} A_x e^{-\frac{\delta}{2}i} \\ A_y e^{\frac{\delta}{2}i} \end{pmatrix}, \quad (1)$$

where $\delta = \delta_y - \delta_x$ is the phase difference, $\tan\alpha = A_y / A_x$ is ratio of amplitudes, and ρ is a newly adapted parameter for revised Jones Matrix which indicate variation of x and y direction's weight depend on applied electric field strength.

Then the light intensity is expressed with ρ.

$$\begin{aligned} I &= |E_x|^2 + |E_y|^2 \\ &= \frac{1}{8}\{(1-\rho^2)\cos^2\alpha - (\rho^2 - 1)\sin^2\alpha\}\cos 4\theta + \frac{1}{4}\{\cos\alpha\sin\alpha(1-\rho^2)\cos\delta\}\sin 4\theta \\ &+ \frac{1}{2}\{\cos^2\alpha - \rho^2\sin^2\alpha\}\cos 2\theta + \frac{1}{2}\{\cos\alpha\sin\alpha(1+\rho^2)\cos\delta\}\sin 2\theta \\ &+ \frac{1}{8}\{3+\rho^2\}\cos^2\alpha + \frac{1}{8}\{3\rho^2 + 1\}\sin^2\alpha \,. \end{aligned} \quad (2)$$

The experimental results are fitted by using of equation (2). Fig.5 is the example of fitting.

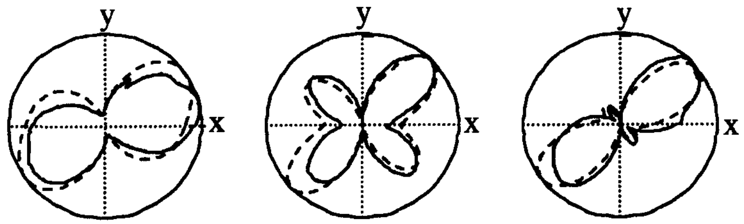

(a) 3V (b) 7V (c) 8V

FIGURE 5. Example of fitting: solid line is experimental results and dashed line is fitting curves.

From the phase difference δ, the average birefringence Δn is obtained, and refractive index of extraordinary light $n_e(\phi) = \Delta n + n_o$ is obtained. As a result, average angle ϕ of tilted director from substrate normal is easily obtained from the relation of

$$\frac{\sin^2\phi}{n_e^{\ 2}} + \frac{\cos^2\phi}{n_o^{\ 2}} = \frac{1}{n_e(\phi)^2} \, . \tag{3}$$

The material parameters of CCH-3 were used n_o=1.4583 and n_e = 1.5041 at 75 °C, which was precisely determined based on measurements carried out in our laboratory. The applied electric field dependence of ϕ is shown in Fig. 6. From Fig. 6, it was found that ϕ is divided three region (A) linear, (B) critical and (C) constant Magic Angle 54.7°, which means completely disorder of director angle.

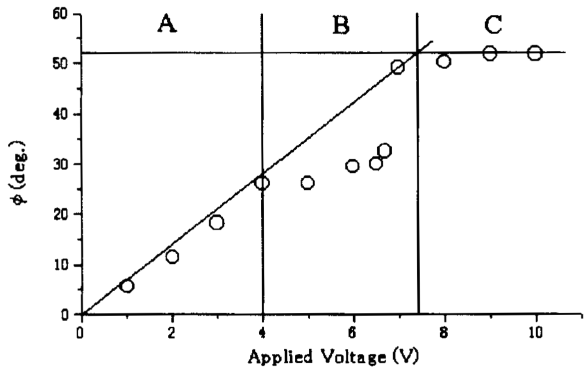

FIGURE 6. Applied electric field dependence of average angle of tilted director ϕ is divided three regions (A) linear, (B) critical and (C) constant.

3 THEORETICAL DISCUSSION

We now wish to solve for the angle of tilted director $\phi(x,z)$ in the interdigital electrode cell by continuum theory for the nematic liquid crystal. In the present geometry, the applied electric field produces a spray deformation mode. The free-energy density in external electric fields can be written as

$$g(r,t) \approx g_{elas} + g_{flexo} + g_{diel} \quad , \tag{4}$$

where the elastic term

$$g_{elas} = \frac{1}{2}K_s(\nabla \cdot n)^2, \tag{5}$$

the flexoelectric term

$$g_{flexo} = -\{e_s(\nabla \cdot n)n\} \cdot E \,, \tag{6}$$

and the dielectric term

$$g_{diel} = -\frac{1}{2}\Delta\varepsilon(E \cdot n)^2 . \tag{7}$$

The constants in g (r,t) are the splay elastic constant K_s, the splay flexoelectric constant e_s and the dielectric anisotropy $\Delta\varepsilon$. Now the director field and the applied electric field can be written as n(r,t)=(sinϕ (x,z),0,cosϕ (x,z))
„and E(r,t)=(E_x(x,z),0,E_z(x,z)) respectively. By using approximation $n_x = \sin\phi \approx \phi$,

$n_z = \cos\phi \approx 1$ ($\phi << 1$) and neglecting the higher differential terms,

$$\begin{aligned} g_{elas} &= \frac{1}{2}K_s\{\cos^2\phi(\frac{\partial\phi}{\partial x})^2 - 2\cos\phi\sin\phi(\frac{\partial\phi}{\partial x})(\frac{\partial\phi}{\partial z}) + \sin^2\phi(\frac{\partial\phi}{\partial z})^2\} \\ &\approx \frac{1}{2}K_s(\frac{\partial\phi}{\partial x})^2, \end{aligned} \tag{8}$$

$$\begin{aligned} g_{flexo} &= -e_s\{(\cos\phi\sin\phi\frac{\partial\phi}{\partial x} - \sin^2\phi\frac{\partial\phi}{\partial z})E_x + (\cos^2\phi\frac{\partial\phi}{\partial x} - \sin\phi\cos\phi\frac{\partial\phi}{\partial z})E_z\} \\ &\approx -e_s\frac{\partial\phi}{\partial x}E_z, \end{aligned} \tag{9}$$

$$g_{diel} = -\frac{1}{2}\Delta\varepsilon(\sin^2\phi E_x{}^2 + 2\sin\phi\cos\phi E_x E_z + \cos^2\phi E_z{}^2)$$

$$\approx -\Delta\varepsilon\phi E_x E_z, \tag{10}$$

are obtained. By using the boundary condition $\phi(-d/2, z) = \phi(d/2, z) = 0$ and the relation of $\nabla \times E = 0$, the free energy per unit area of the interdigital electrode cell can be written as

$$G(r) = \int g(r)dr$$

$$= \int_{-\frac{d}{2}}^{\frac{d}{2}} \int_0^P \{\frac{1}{2}K_s(\frac{\partial\phi}{\partial x})^2 - e_s \frac{\partial\phi}{\partial x}E_z - \Delta\varepsilon\phi E_x E_z\} dxdz$$

$$= \iint \{\frac{1}{2}K_s(\frac{\partial\phi}{\partial x})^2 + e_s\phi\frac{\partial E_z}{\partial x} - \Delta\varepsilon\phi E_x E_z\} dxdz. \tag{11}$$

From variational principle, we can derive Euler-Lagrange's equation

$$K_s \frac{\partial^2\phi}{\partial x^2} = e_s \frac{\partial E_z}{\partial x} - \Delta\varepsilon E_x E_z. \tag{12}$$

This equation is linear in ϕ and the general solution can therefore be obtained as linear superposition of solution in witch the flexoelectric and dielectric coupling are treated separately.

Following Prost and Pershan, the electric fields that result from the interdigital electrode can be written as

$$E_x(x,z) = \mathrm{Re}[-\frac{\pi V}{\sqrt{2}Gd}\{\cos(\frac{2\pi\xi}{d})\}^{-\frac{1}{2}}], \tag{13}$$

$$E_z(x,z) = -\mathrm{Im}[-\frac{\pi V}{\sqrt{2}Gd}\{\cos(\frac{2\pi\xi}{d})\}^{-\frac{1}{2}}] \quad , \tag{14}$$

where $\xi = x + iz$, $G = F(2^{-1/2}, 1)$ and $F(k,u) = \int_0^u [(1-v^2)(1-k^2v^2)]^{-1/2} dv$ is the elliptic integral of the first kind. The electric fields that result from the interdigital electrode are shown in Fig. 7. This future was confirmed already by the water tank electric potential field experiment in our laboratory.

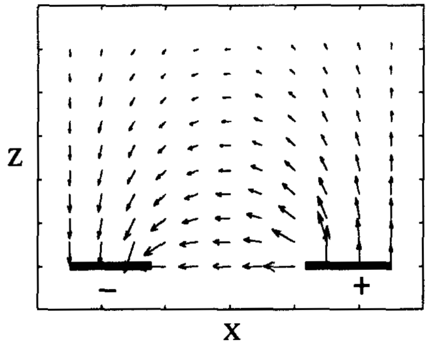

FIGURE 7. The electric fields that result from the interdigital electrode. An arrow represents electric field vector E (x,z).

Equation (12) could be solved using numerical analysis. The applied voltage dependence of ϕ (x,z) for flexoelectric effect is shown in Figure 8.

In its initial state (Fig. 8 (a)), the director field has homeotropic geometry. The applied electric field dependence of director field is divided three regions. First, when applied electric field is weak (Fig. 8 (b)), the tilted angle is linear in applied electric field and the director field in this region is linear normal state. It is equivalent to the linear region in Fig. 6 (A). Second, when applied electric field is middle (Fig. 8 (c)), the director field has a small winding near the electrode. Its average tilted angle of director is nonlinear abnormal state by the applied electric field. It is equivalent to the critical region in Fig. 6 (B). Finally, when applied electric field is strong (Fig. 8 (d)), director field is perfectly at random and it is equivalent to the constant region in Fig. 6 (C).

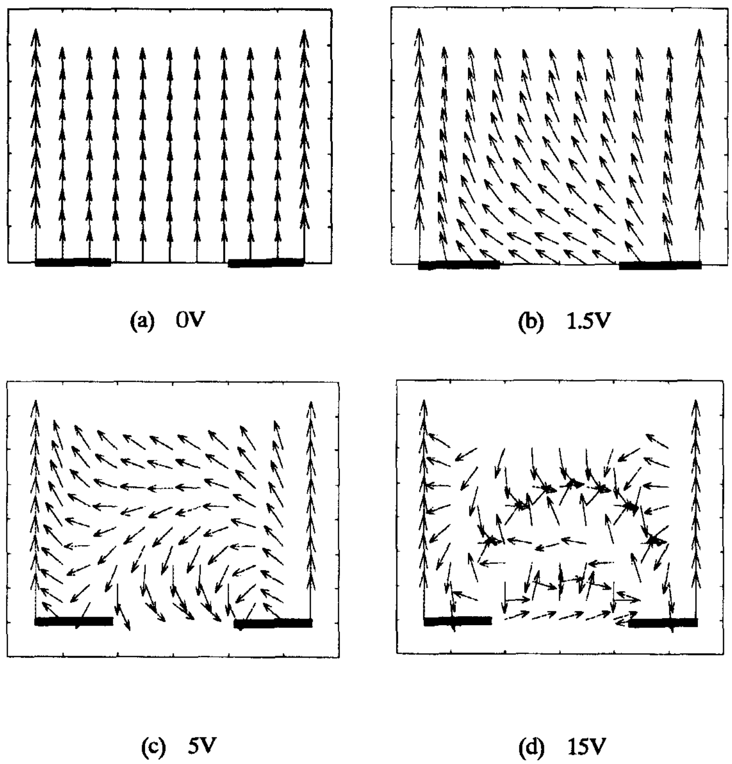

FIGURE 8. The dependence of applied electric field of director distribution. An arrow represents a director vector n (x,z).

4 SUMMARY

By interdigital electrode method, flexoelectric splay deformation of CCH nematic liquid crystal was precisely investigated.

Polarization characteristics of Fraunhofer diffraction for splay type flexoelectric effect were analyzed by revised Jones matrix method. The applied electric field dependence of average angle of tilted director is divided three regions (linear, critical, and constant) and constant region has Magic Angle 54.7°, which means completely disorder of director.

According to numerical simulation based on continuum theory, the physical meaning of experimental results in these three regions was explained by splay type flexoelectric effect; the applied electric field dependence of director field is divided three regions at threshold values. When applied electric field is weak, director field have uniform deformation. This deformation represents linear flexoelectric effect. When applied electric field is middle, the director have locally winding near electrode, and when applied electric field is strong, director field is perfectly disorder. In this region, splay deformation destroy linearity of flexoelectric effect.

Therefore if we detect linearity of flexoelectric effect quantitatively, we pay attention to strength of electric field under the threshold value for splay type flexoelectric effect.

References

[1] R.B. Meyer; Phys. Rev. Lett., **22**, 918, (1969).
[2] D. Schmidt, M. Schadt and W. Helfrich; Z. Naturforsch., **27 a,** 277, (1971).
[3] I. Dozov, Ph. Martinot-Lagarde and G. Durand; J. Physique Lett., **43**, L-365, (1982).
[4] J. Prost and P.S. Pershan; J. Appl. Phys., **47**, 2298, (1976).